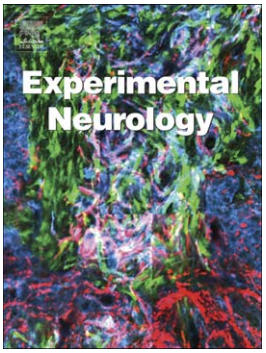

Consequences of excessive plasticity in the hippocampus induced by perinatal asphyxia

G.E. Saraceno, L.G. Caceres, L. Guelman, R. Castilla, L.D. Udovin, M.H. Ellisman, M.A. Brocco, F. Capani

PII: S0014-4886(16)30257-6
DOI: doi: 10.1016/j.expneurol.2016.08.017
Reference: YEXNR 12392

To appear in: *Experimental Neurology*

Received date: 1 April 2016
Revised date: 21 August 2016
Accepted date: 26 August 2016

Please cite this article as: Saraceno, G.E., Caceres, L.G., Guelman, L., Castilla, R., Udovin, L.D., Ellisman, M.H., Brocco, M.A., Capani, F., Consequences of excessive plasticity in the hippocampus induced by perinatal asphyxia, *Experimental Neurology* (2016), doi: 10.1016/j.expneurol.2016.08.017

CONSEQUENCES OF EXCESSIVE PLASTICITY IN THE HIPPOCAMPUS INDUCED BY PERINATAL ASPHYXIA

Saraceno G. E. [(1)] †,Caceres L.G. [(2)], Guelman L. [(2)], Castilla R. [(1)], Udovin L.D. [(1)], Ellisman MH, [(3)], Brocco, M.A. [(4)]Capani F. [(1,5)§].

[(1)] ININCA, Universidad de Buenos Aires (UBA)-CONICET, Buenos Aires, Argentina.
[(2)] Facultad de Medicina (UBA) CEFyBO-CONICET, Buenos Aires, Argentina.
[(3)] Department of Neuroscience, National Center for Electron Microscopy and Imaging Research, UCSD.
[(4)] Instituto de Investigaciones Biotecnológicas-Instituto Tecnológico de Chascomús (IIB-INTECH). UNSAM-CONICET, Buenos Aires, Argentina.
[(5)] Instituto de Ciencias Biomédicas, Facultad de Ciencias de la Salud, Universidad Autónoma de Chile, Chile.

[§]Correspondingto: Instituto de Investigaciones Cardiológicas "Prof. Dr. Alberto C. Taquini" (ININCA), UBA-CONICET, Marcelo T. de Alvear 2270, C1122AAJ, Buenos Aires, Argentina. Phone/Fax: +5411 4508 3880/8. fcapani@fmed.uba.ar (Capani F.).

†Currentaddress: Interdisciplinary Institute for Neuroscience, UMR 5297, Centre National de la Recherche Scientifique (CNRS), Bordeaux, France

Running title: Perinatal asphyxia increased hippocampal synaptogenesis

Word count: Abstract: 240. Keywords: 6. Entire manuscript excluding legends and references: 3931. Figures: 5. Total number of pages: 20.

ABSTRACT

Perinatal asphyxia (PA) is one of the most frequent risk factors for several neurodevelopmental disorders (NDDs) of presumed multifactorial etiology. Dysfunction of neuronal connectivity is thought to play a central role in the pathophysiology of NDDs. Because underlying causes of some NDDs begin before/during birth, we asked whether this clinical condition might affect accurate establishment of neural circuits in the hippocampus as a consequence of disturbed brain plasticity. We used a murine model that mimics the pathophysiological processes of perinatal asphyxia. Histological analyses of neurons (NeuN), dendrites (MAP-2), neurofilaments (NF-M/Hp) and correlative electron microscopy studies of dendritic spines were performed in *Stratum radiatum* of the hippocampal CA1 area after postnatal ontogenesis. Protein and mRNA analyses were achieved by Western blot and RT-qPCR. Behavioral tests were also carried out. NeuN abnormal staining and spine density were increased. RT-qPCR assays revealed a β-actin mRNA over-expression, while Western blot analysis showed higher β-actin protein levels in synaptosomal fractions in experimental group. M6a expression, protein involved in filopodium formation and synaptogenesis, was also increased. Furthermore, we found that PI3K/Akt/GSK3 pathway signaling, which is involved in synaptogenesis, was activated. Moreover, asphyctic animals showed habituation memory changes in the open field test. Our results suggest that abnormal synaptogenesis induced by PA as a consequence of excessive brain plasticity during brain development may contribute to the etiology of the NDDs. Consequences of this altered synaptic maturation can underlie some of the later behavioral deficits observed in NDDs.

Highlights:

- We study how excessive plasticity induced by PAaffects hippocampus development.
- Dendritic spines density and synaptogenesis are altered by excessive plasticity.
- Habituation memory changes were observed in asphyctic animals.

Keywords: Neurodevelopmental disorders; M6a; PI3K/Akt/GSK3 pathway; habituation memory; β-actin; synaptogenesis.

Abbreviations: NDDs: neurodevelopmental disorders; PA: perinatal asphyxia; GFAP: glial fibrillary acidic protein; MAP-2: Microtubule associate protein-2; NF H/Mp: phosphorylated high and medium molecular weight neurofilaments; NeuN: neuron-specific nuclear protein; OF: Open field test; LC: number of lines crossed; CE: center entries; PI3K: Phosphatidylinositol-4,5-bisphosphate 3-kinase; GSK3: glycogen synthase kinase 3.

INTRODUCTION

Age-dependent symptom onset is a key characteristic of several neurodevelopmental disorders (NDDs). Different stressors ("factors") during perinatal life could induce abnormalities in brain development which may produce long-lasting deleterious consequences in adult brain functioning (Basovich, 2010). A substantial body of evidences has already shown that the developing brain is susceptible to hypoxia-ischemia in spite of its enhanced capacity for brain plasticity (Johnston, 2004). Perinatal asphyxia (PA) has been largely associated with NDDs of presumed multifactorial etiology, in which certain aspects of neurodevelopment are selectively impaired during a period of apparent normal development (van Handel et al., 2007).

During neuronal development, thin and highly motile dendritic filopodia could transform into more stable dendritic spines (Yoshihara et al., 2009), playing a crucial role in building neural circuits (Matus, 2000). In the last few years was shown that M6a over-expression induces neurites formation and a higher filopodium/spine density in rat hippocampal primary cultures (Alfonso et al., 2005) and participates in synaptogenesis (Brocco et al., 2003), processes in which PI3K/Akt/GSK3 pathway activation plays a key role (Cuesto et al., 2011). Modifications in actin cytoskeleton regulation of hippocampal dendritic spines were described in different memory disorders (Newey et al., 2005). Several studies have proposed that this brain region could be involved in the pathophysiology of NDDs (Harrison, 2004; Rojas et al., 2004).

Previous studies have shown that aberrant neurogenesis leads to abnormal neural network formation (Colon-Ramos, 2009). Although numerous researches have mainly analyzed the mechanisms of cell death or survival (Morales et al., 2008), there is not enough data that explain how PA could be involved in the physio-pathogenesis of NDDs. Following the hypothesis that excessive plasticity in the developing brain could lead to

disability through reorganization of new maladaptive neuronal circuits (Johnston, 2011), we worked in a murine model that mimics the pathophysiological processes of PA at the time of delivery to a closer extent (Pokorny and Yamamoto, 1981) to provide biochemical, morphological and behavioral analyses of how PA affects synaptogenesis and dendritic spine density after postnatal ontogenesis of CA1 hippocampal.

MATERIALS AND METHODS

Animals and perinatal asphyxia model

All animal´s procedures were approved by the Institutional Animal Care and Use Committee at the University of Buenos Aires (CICUAL#4091/04) and conducted according to the principles of the Guide for the Care and Use of Laboratory Animals (Animal Welfare Assurance, A-3033-01/protocol#S01084). Eighteen full-terms pregnant Sprague Dawley rats on gestational day 22 were individually observed and when no more than two pups were delivered, the dam was immediately euthanized by decapitation and the uterus horns were rapidly isolated through an abdominal incision. The uterus horns were placed in a water bath at 37°C for 19 min (moderate to severe PA) (Galeano et al., 2011). Following PA, uterus horns were opened, pups were removed and stimulated to breathe by performing tactile intermittent stimulation with pieces of medical wipes until regular breathing was established. Umbilical cord was tied and the animals were left to recover for 1h under a heating lamp. When their physiological conditions improved, they were given to surrogate mothers (n=12) that had delivered normally within the last 24h. The different groups of pups were marked and mixed with the surrogate mothers' normal litters (control animals that were left undisturbed, 10 pups in total). Cesarean controls were not used due to previous study showed no significant alterations compared with undisturbed animals (Galeano et al., 2011). All experiments were performed in male animals.

Tissue fixation, immunohistochemistry and immunofluorescence

Intracardiac perfusion and coronal hippocampal sections were performed as described previously (Capani et al., 2001; Galeano et al., 2011; Saraceno et al., 2010). Free-floating sections were incubated overnight at 4°C with anti-neuron-specific nuclear protein (NeuN; 1:1000, mouse-IgG; Millipore), anti-microtubule-associated protein 2 (MAP-2; 1:250, mouse-IgG; Sigma-Aldrich), anti-phosphorylated high and medium molecular

weight neurofilaments (NF H/Mp; 1:500, rabbit-IgG; Millipore) or anti-phosphorylated Akt (p-Akt1/2/3 (Ser 473)-R, rabbit polyclonal; Santa Cruz). Then sections were incubated for 2h at room temperature (RT) with secondary antibodies (Biotinylated anti-mouse-IgG, 1:300, Vector; Biotinylated anti-rabbit-IgG, 1:300, Vector). Amplification was done using avidin-biotinylated horseradish peroxidase complex (ABC; Vector) in PBS for 1h, followed by washing in PBS before chromogen development (DAB; Vector). Immunofluorescence was performed on free-floating sections as described previously by Saraceno et al. (2010). Sections were incubated overnight at 4°C with a rat polyclonal anti-M6a antibody (1:100; Medical and Biological Laboratories), anti-Glial fibrillary acidic protein (GFAP; rabbit-IgG, 1:2000, Dako) or phalloidin-Alexa568 (Molecular Probes). Then sections were incubated for 2h at RT with Alexa546 goat anti-rat-IgG (1:200, Molecular Probes), counterstained with DAPI and mounted with Vectashield mounting medium (Vector). Light images were obtained using an E600 microscope equipped (Nikon) and confocal images using a SP5X Confocal Microscope (Leica).

Photooxidation

Electron microscopic distribution of filamentous actin (F-actin) in the rat hippocampus (n=3 per group) using phalloidin conjugated with eosin was performed as was described in previous paper (Capani et al., 2001). In few words, vibratome sections were washed with 50mM glycine-PBS containing 0.5% cold water fish gelatin to block nonspecific binding. Following 30 min of washing, the sections were incubated on a shaker, in a solution of 0.05% of eosin phalloidin-0.5% cold-water fish gelatin/50mM glycine-PBS for 2 h at 4ºC. For light microscopic studies, phalloidin conjugated to Alexa488 was also used because of its superior fluorescent quantum yield compared to eosin. As a negative control, eosin-phalloidin was omitted. Tissue sections stained with eosin-phalloidin were mounted on glass-welled tissue culture dishes (Mat Tek Corp) pretreated with polyethylenimine. The slices were fixed again for 2–5min with 2% glutaraldehyde in 0.1M cacodylate buffer, rinsed in buffer for several minutes, and placed in 50mM glycine and potassium cyanide in cacodylate buffer for an additional 5 min to reduce nonspecific staining. Photooxidation was performed on the Zeiss Axiovert described above, equipped with a 75-W xenon arc light source. The samples were immersed in a solution of 2.8mMdiaminobenzidine in 0.1M sodium cacodylate at 4ºC bubbled with pure

O_2, final pH 7.4, and then irradiated under conventional epifluorescence using a xenon lamp. After 6–8 min, a brownish reaction product began to appear in place of the fluorescence. The process was stopped by halting the excitation. We analyzed 603 control spines and 621 spines from tissue subjected to PA.

Morphometric analysis the point-counting method

Morphometric analysis was performed according to the methodology described in previous paper (Saraceno et al., 2010). Volume fraction of immunoreactive material for MAP-2, NF H/Mp and phalloidin-Alexa^{568} were estimated using the point-counting method and a grid delimiting 5000 μm^2 in the *Striatum radiatum* of CA1. A total area of 75,000 μm^2 was evaluated in each animal. Percentage of reactive area was estimated using Image J Program (Image J 1.41o, NIH). The number of GFAP immunoreactive astrocytes was estimated in the Stratum radiatum of CA1 hippocampal area. A total of 80 counting frames were assessed per animal. Section thickness was measured using a digital length gauge device (Heidenhain-Metro MT 12/ND221; Traunreut, Germany) attached to the stage of a Leitz microscope. Cell nuclei from GFAP immunoreactive cells that came into focus while focusing down through the dissector height were counted. All counts were performed on coded sections. The volume of the striatum radiatum of CA1 was estimated using the point counting method of Weibel (1979).

Immunoblotting

Subcellular fractionation was performed as previously described (DiGiovanni et al., 2012). Dounce homogenates of the pellets in ice cold TEVP buffer (10mMTris- HCl, pH 7.4, 5mMNaF, 1mM Na3VO4, 1mM EDTA, and 1mM EGTA, 1.25 μg/mL pepstatin A, 10 μg/mL leupeptin, 2.5 μg/mL aproptionin, 0.5mM PMSF) containing 320mM sucrose were centrifuged at 1000 × g to remove nuclei and large debris. The supernatant was centrifuged at 10.000 × g for 10min to obtain a crude synaptosomal fraction and subsequently was lysed hypoosmotically and centrifuged at 45.000 × g for 90min to obtain a pellet of the synaptosomal membrane fraction. After each centrifugation, the resulting pellet was rinsed briefly with ice cold TEVP buffer before subsequent fractioning to avoid possible crossover contamination. Protein concentration was estimated by Bradford technique.

Synaptosomal membrane fraction (n=5 per group) were incubated overnight at 4°C with anti-β-actin (1:3000, mouse-IgG, Sigma-Aldrich). Membranes containing cytoplasmic

fractions (n=5 per group) were then incubated overnight at 4°C with anti-Akt (1:1000, mouse-IgG, Cell Signaling), anti-GSK3-beta antibody (1:500, mouse-IgG, Abcam), anti-phospho-Akt-Thr308 (p-Akt, 1:1000,rabbit-IgG, Cell signaling), anti-GSK3 beta-phospho S9 (GSK3β-p-Ser, 1:500,rabbit-IgG, Abcam), anti-Glial fibrillary acidic protein (GFAP; rabbit-IgG, 1:2000, Dako). We use anti glyceraldehyde-3-phosphate dehydrogenase (GAPDH, 1:1000, rabbit-IgG, Sigma-Aldrich) as loading control. Blots were rinsed three times in PBS with 0.5% Tween-20 buffer (PBST), and then incubated with the corresponding horseradish peroxidase (HRP)-conjugated secondary antibody (1:1000, Bio-Rad) for 2h at RT. Immunoreactive bands were detected using an ECL™ Western Blotting Analysis System (Amersham™, GE/Healthcare). Films were scanned and the optical density of protein bands was quantified using Gel Pro Analyzer software 3.1.00.00 (Media Cybernetics).

Real time quantitative PCR (RT-qPCR)

Hippocampi (n=12 per group) were homogenized in TRIzol® reagent (Invitrogen) using a tissue homogenizer. Total RNA was isolated from TRIzol® homogenates following manufacturer's protocol. Poly(A)+ RNA was purified from total RNA using the PolyATract mRNA Isolation System (Promega) as previously described (Brocco et al., 2003). mRNA was transcribed using Superscript II enzyme (Invitrogen) following the manufacturer's instructions. RT-qPCR reactions were carried out in an Applied Biosystems 7500 Real-Time PCR System (Applied Biosystems). Primer sequences were designed using Primer Express software (Applied Biosystems). Amplicons were 60-100 bp long. Oligonucleotide forward primers sequences used were: 5'AAATAATGATGTAGCCTGACAAGAAATTT3', 5´CAACTTGATGTATGAAGGCTTTTGGT3´and5'AAGCATACAGGTCCTGGCATCT 3', and reverse primers 5'AATGCACTTACACTGAAGGAGGAAT3', 5´ACTTTTATTGGTCTCAAGTCAGTGTACAG3´and5'CATTCAGTCTTGGCAGTGC AG3', for gpm6a, β-actin and cyclophilin, respectively. Reactions were carried out with the SYBR®GREEN PCR Master Mix (Invitrogen) as described previously (Brocco et al., 2003). All the samples were tested against cyclophilin as reference gene for data normalization (Cattano et al., 2010). Each RT-qPCR quantitation experiment was done in triplicates for three independently generated cDNA templates.

Behavioral tests.

All experimental experiments were carried out in an isolated behavioral room, between 11 AM to 4 PM.

Open Field test

Experiments were carried out as described by Caceres et al. (2010). The total number of lines crossed, latency to and number of entries to the center and frequency and duration of grooming were recorded using a digital video camera. Grooming behavior was separated in its sequential components, similarly as it has been carried out elsewhere. Phase I includes rapid elliptical forepaw strokes around the nose and vibrissae while phase II includes small unilateral and/or large bilateral strokes over face and head by one or both paws, body licking of the ventrolateral torso and genitals. All these parameters were expressed as a percentage of total grooming duration. Comparisons between behaviors displayed by the groups during the first session (when novelty is maximal) and during the second session (when animals normally exhibit acclimatization to the environment) to evaluate habituation memory were performed. Activity was recorded using a camcorder (JVC Everio GZ-HD620 or Sony DCR-SR47 Handycam with Carl Zeiss optics). To minimize olfactory cues, the apparatus was cleaned with a 70% ethanol solution between sessions.

Inhibitory avoidance test

Inhibitory avoidance (IA) task measures the memory of an aversive experience through the simple avoidance of a location in which the unpleasant experience occurred. This task depends heavily on the dorsal hippocampus (Lorenzini et al., 1996). We used an IA apparatus as described by Roozendaal et al. (2002). Experiments were conducted as described by Caceres et al. (2010).

Statistical analysis

Data was analyzed for each experimental group and for each parameter studied. The results were expressed as the means ± SEM. Student's t-test were conducted. For behavioral analyzes, one-way analysis of variances (ANOVAs) followed by post-hoc multiple comparisons (Fisher´s test) were carried out. A probability was considered significant at 5% or less. Two-tailed probabilities were always reported. Statistical analyses

were performed using the GraphPad Prism 5.03 statistical package for Windows (GraphPad software).

RESULTS

Vulnerability of pyramidal hippocampal neurons

We classified NeuN+ neurons in two categories: a) normal neurons, characterized by an intense NeuN+ nucleus and b) abnormal neurons, with NeuN fragmentation of the nucleus, or cytoplasmic staining without nuclear staining (Robertson et al., 2006). We observed a significant increase in the number of abnormal neurons in the hippocampal CA1 layer of asphyctic animals (Fig. 1a and b). Electron microscopy analyses showed clear degeneration of CA1 hippocampal pyramidal neurons. In addition, when we evaluated the morphological changes of GFAP positive astrocytes and the expression of this protein, we did not observe any difference between groups (Fig. 1 and Fig. 4, respectively). Altogether, these results indicate that major PA effects occurred on CA1 neurons.

Since PA affected neuronal population, we also studied cytoskeleton organization of neural processes. Changes in dendrite morphology were analyzed through a dendrite-specific marker MAP-2 immunostaining. We did not find any significant alterations in dendrite morphology or in the percentage of reactive area between groups (Supplemental material Fig. 1a). We also analyzed by immunostaining the presence of phosphorylated medium and heavy neurofilaments (NF H/Mp) as a measure of axonal dysfunction and degeneration (Saraceno et al., 2010). No significant differences between experimental groups were observed (Supplemental material Fig. 1b).

Effects of perinatal asphyxia on post-synapses

Mature dendritic spines, structures susceptible to hypoxic insults (Saraceno et al., 2012), contain a β-actin-rich cytoskeleton. Thus, we analyzed β-actin content within dendritic spines to examine the magnitude of PA-induced damage. While mRNA encoding actin is located in the neuronal cell body, β-actin protein is concentrated in dendritic spines (Kaech et al., 1997). Thence, we quantified β-actin mRNA by RT-qPCR and protein levels by Western blot of hippocampal tissue samples and hippocampal synaptosomal fractions

respectively. PA significantly increased β-actin mRNA expression in hippocampal tissue (Fig. 2a). Moreover, Western blot analysis showed a significant increase in β-actin levels in synaptosomal fractions of asphyctic animals (Fig. 2b).

We analyzed actin filament content (F-actin) in hippocampus slices to estimate spine density using the actin-binding toxin phalloidin (Capani et al., 2001). Dot intensity was detected at the confocal (Alexa^{568}-conjugates) and electron microscopic (photooxidation) levels and was used as a measure of dendritic spine density. In the asphyctic group, quantitative analysis of confocal microscopy observations showed that phalloidin-Alexa^{568} stained reactive area significantly increased in the *Stratum radiatum* of hippocampal CA1 layer (Fig. 2c). We estimated the number of dendritic spines by studies of F-actin distribution using correlative photooxidation (Capani et al., 2001). Statistical analysis of photooxidated samples showed a significant increase in the number of phalloidin-positive dendritic spines in experimental group.

In a detailed analysis by photooxidation technique, we observed an increase in filopodial structures density in asphyctic animals (Fig. 3a). Since M6a overexpression in rat primary hippocampal neurons in culture induces the formation of filopodium-like protrusions that could act as spine precursors (Brocco et al., 2010), we studied M6a modifications in PA animals. RT-qPCR measurements of the *gpm6a* mRNA expression in the hippocampus showed a significant increase in asphyctic rats (Fig. 3b). In hippocampal slices, M6a immunoreactivity quantification showed a significant increase in asphyctic group (Fig. 3c). Taken together these data suggest that PA may affect spine density.

Perinatal asphyxia increased PI3K/Akt/GSK3 signaling pathway activity

Functional synaptogenesis and spine density increment induced by PI3K/Akt/GSK3 pathway activation have been described in hippocampal neurons (Cuesto et al., 2011; Kwon et al., 2006). Therefore, we investigated by Western blot this pathway activation in hippocampal cytoplasmic fractions. Considering that Akt is the major target of PI3K activation, we studied the presence of Akt activated form (p-Akt) and of glycogen synthase kinase 3 (GSK3), one of the downstream pathway components. While the total amount of either Akt or GSK3 protein was not altered, we found a significant increase of p-Akt levels in asphyctic animals (Fig. 4). In addition, a small increase of GSK3-p-Ser9 was observed in

asphyctic animals (Fig. 4), indicating a down-regulation of its activity. In addition, we performed an immunohistochemistry to determinate the p-Akt location. We could deduce that the boost of Akt activity is more concentrated in neurons, according with previous studies (Cuesto et al., 2011) (Fig. 4, inset).

Asphyctic animals showed habituation memory changes

Since PA affects spine density, we investigated the consequences on learning and memory processes through different behavioral tests. Although both groups showed a significantly locomotor habituation response in the open field test (OF), asphyctic animals showed a more pronounced number of lines crossed (LC) decrement in the second test exposure compared with controls animals(Fig. 5a). Considering anxiety-related behaviors, no differences were observed between groups (supplemental material Fig. 2).

When we analyzed the duration and frequency of grooming in order to evaluate the involvement of this behavior in the habituation process, PA group showed a significant increase in both parameters during the second exposure to the OF (Fig. 5b and 5c). In addition, we divided the grooming pattern of the second exposure in two phases for a better analysis (see Materials and Methods section).We observed that phase I was significantly shorter while phase II was significantly longer in asphyctic animals indicating they are de-aroused from novelty and disengaged from exploratory and vigilance activities (Fig. 5d). To determine whether locomotor activity and grooming behavior were mutually involved in OF habituation, a regression analysis was performed. We found a correlation between total grooming duration and locomotor activity (measured as the number of LC, Fig. 5e), and phase II duration and locomotor activity in asphyctic animals (Fig. 5f). In contrast, no association between crossing and grooming was observed in control group. These results suggest grooming behavior as a factor that would be taking part in the open field habituation process of asphyctic animals. We also analyzed associative memory using inhibitory avoidance test and found no significant differences (T2/T1 ratio, supplemental material, Fig. 3).

DISCUSSION

We present novel evidence about how the interruption of normal brain development by perinatal asphyxia promotes hippocampal synaptogenesis inducing an increase of dendritic spine density in the hippocampal CA1 *Stratum radiatum*during development. This is well correlated with behavioral changes such as a greater response to the habituation behavior to an open field test and precedes neurodegenerative modifications observed after 2 and 4 months of the asphyctic insult (Saraceno et al., 2010, 2012; Muñiz et al 2014). Several efforts have been made the last years to design novel therapeutical tools to reduce the rate and severity of neurodevelopmental disabilities resulting from PA. These findings could help to determine a time window of high brain susceptibility to therapies/treatments (Meredith et al., 2012) during brain development and underlying NDDs.

Astrocytic role in NDDs has gained significance in the last years (McGann et al., 2012). Although enhanced GFAP staining and gliosis could persist in association with neuronal loss (Ordy et al.,1993), no significant differences neither in the number of GFAP astrocytes/mm3 or in GFAP expression were observed between groups one month after the injury in this work. Previous work showed evident reactive gliosis in the CA1 hippocampal area of four month-old asphyctic animals (Saraceno et al., 2010), positing that changes in glial population may be progressive and sustained after long-time of PA. In addition, clinical imaging studies have confirmed the presence of reactive gliosis in different brain areas from seven months-old patients that suffered PA (Huang et al., 2008).

Most of the spines are thought to arise from dendritic filopodial during early postnatal life (Ziv and Smith, 1996; Yoshihara et al., 2009). *In vitro* studies have shown that filopodia are active along dendritic lengths during postnatal synaptogenesis in CA1 hippocampal area (Fiala et al., 1998). This spread in filopodium/dendritic spine density is closely associated among others with increased expression of the glycoprotein M6a, which is involved in filopodium and synapse formation (Alfonso et al., 2005; Brocco et al., 2010). A substantial body of evidence have shown that prenatal stress also induced an increase in M6a mRNA expression (Martinez-Tellez et al., 2009; Mychasiuk et al., 2012; Monteleone et al., 2013), suggesting that stressful situations during early stages of life induced similar changes in *gpm6a* mRNA levels.

Previous *in vivo* and *in vitro* studies have supported a direct role of PI3K/Akt/GSK3 signaling pathway in synaptogenesis regulation (Cuesto et al., 2011) and dendritic

development (Cosker and Eickholt, 2007). In addition, alterations in the Akt pathway have been also related to several neurodegenerative diseases (Griffin et al., 2005). While GSK3 overexpression reduces the synapse number, GSK3 down-regulation increases axonal growth and synaptic terminals number (Pokorny and Yamamoto, 1981). Accordingly, our results suggest an Akt up-regulation, mainly in CA1 pyramidal cells, and a down-regulation of GSK3 activity in asphyctic animals, probably as a consequence of Ser9 phosphorylation induced by Akt. Since we observed *in vivo* supernumerary spines in hippocampal neurons and increased glycoprotein M6a expression, our data suggests that PI3K/Akt/GSK3 pathway could be one of the signaling pathways involved in spine density regulation in asphyctic animals (Cuesto et al., 2011).

Several neurological disorders affecting memory involve defects in the actin cytoskeleton regulation of dendritic spines (Newey et al., 2005). Corbett et al., (2006) suggested a correlation between dendritic spine density and an increased Open Field habituation. Continuous exposure to the same environment induces a reduction in exploratory behavior (Barros et al., 2006). Our results have shown that the PA group exhibited a greater response to the habituation behavior to an OF. In the same line, a recent study described that asphyctic rats showed impaired recognition and spatial reference memory at the same age (Blanco et al., 2015). On the other hand, no significant modifications in the anxiety-related behaviors were observed, consistent with other studies in which no modifications in anxiety-related behaviors were seen at 3 months of age in asphyctic animals (Galeano et al., 2011). Furthermore, asphyctic animals showed no alterations in the short-term memory measured in the inhibitory avoidance task, indicating that PA has not affected associative memory.

Similarly to our previous observations of a significant decrease in the number of normal NeuN+ nuclei at four-month-old animals, here we showed a significant increment in the number of abnormal NeuN stained hippocampal neurons 30 days after PA (Saraceno et al., 2012). However, this alteration was not accompanied by neuronal loss, as we previously showed in several works from our lab using the same PA model (Saraceno et al., 2010, 2012; Blanco et al., 2015). Since Abnormal NeuN+ cells was associated with Tunnel reactivity (Hoffman et al., 2001) and with cresyl violet modification observed in acute brain ischemia (Vereckzy et al., 2006), we think that many of these cells starts in this point

a process of cell death that is evident at 120 after PA (Saraceno et al., 2012) PA. In addition, an increment in apoptosis in the CA1 hippocampal region was demonstrated together with a rise of BAD, BCL-2 and ERK2 protein levels in whole hippocampus 7 and 30 days after 20 min of PA (Morales et al., 2008). While the increment in BAD supports the idea that delayed cell death could occur after PA, BCL-2 and ERK2 modifications suggest the activation of neuroprotective and repair pathways. Our data contributes to the proposed idea that apoptosis is the mechanism that induces adjustment of neuronal population number and/or the elimination of aberrant connections in the pathology of PA-associated disorders (Rami et al., 2003).

Conclusions

Our study reveals a novel impact of the interruption of brain development by perinatal asphyxia, whereby excessive plasticity affects dendritic spine density and synaptogenesis, both involved in neural circuit establishment of rat hippocampus during developing. Taking together these results suggest that abnormal synaptogenesis induced by excessive plasticity during brain development induced by PA may contribute to the etiology of the NDDs.

Conflict of interest

The authors declare that they have no conflicts of interest.

Acknowledgments

GES was a recipient of a post-doctoral fellowship from the Consejo Nacional de InvestigacionesCientíficas y Técnicas of Argentina (CONICET). FC, GL, CR and MAB are career investigators from CONICET. This work was supported by a grant to FC from the CONICET (PIP/2011-2013#11420100100135) and the University of Buenos Aires (UBACyT/2010-2012#20020090100118).

REFERENCES

Alfonso J, Fernandez ME, Cooper B, Flugge G, Frasch AC., 2005. The stress-regulated protein M6a is a key modulator for neurite outgrowth and filopodium/spine formation. Proc Natl Acad Sci U S A. 102:17196-17201.

Barros D, Amaral OB, Izquierdo I, Geracitano L, do Carmo Bassols Raseira M, Henriques AT, Ramirez MR., 2006. Behavioral and genoprotective effects of Vaccinium berries intake in mice. Pharmacol Biochem Behav. 84(2):229-34.

BasovichSN., 2010. The role of hypoxia in mental development and in the treatment of mental disorders: a review. Biosciencetrends. 4:288-296.

Blanco E, Galeano P, Holubiec MI, Romero JI, Logica T, Rivera P, Pavón FJ, Suarez J, Capani F, Rodríguez de Fonseca F. 2015. Perinatal asphyxia results in altered expression of the hippocampal acylethanolamide/endocannabinoid signaling system associated to memoryimpairments in postweaned rats. Front Neuroanat. 9:141.

Brocco M, Pollevick GD, Frasch AC., 2003. Differential regulation of polysialyltransferase expression during hippocampus development: Implications for neuronal survival. J Neurosci Res. 74:744-753.

Brocco MA, Fernandez ME, Frasch AC., 2010. Filopodial protrusions induced by glycoprotein M6a exhibit high motility and aids synapse formation. Eu J Neurosci. 31:195-202.

Caceres LG, Aon Bertolino L, Saraceno GE, Zorrilla Zubilete MA, Uran SL, Capani F, Guelman LR., 2010. Hippocampal-related memory deficits and histological damage induced by neonatal ionizing radiation exposure. Role of oxidative status. Brain Res. 1312:67-78.

Capani F, Martone ME, Deerinck TJ, EllismanMH., 2001. Selective localization of high concentrations of F-actin in subpopulations of dendritic spines in rat central nervous system: a three-dimensional electron microscopic study. J Comp Neurol. 435:156-170.

Cattano D, Valleggi S, Abramo A, Forfori F, Maze M, Giunta F., 2010. Nitrous oxide discretely up-regulates nNOS and p53 in neonatal rat brain. Minerva Anestesiol. 76(6:420-4.

Colon-Ramos DA., 2009. Synapse formation in developing neural circuits. Curr Top Dev Biol. 87:53-79.

Corbett D, Giles T, Evans S, McLean J, Biernaskie J., 2006. Dynamic changes in CA1 dendritic spines associated with ischemic tolerance. Exp Neurol. 202(1):133-8.

Cosker KE, EickholtBJ., 2007. Phosphoinositide 3-kinase signalling events controlling axonal morphogenesis.BiochSoc Trans. 35:207-210.

Cuesto G, Enriquez-Barreto L, Carame´s C, Cantarero M, Gasull X, Sandi C, Ferru´ s A, Acebes A´, Morales M., 2011. Phosphoinositide-3-kinase activation controls synaptogenesis and spinogenesis in hippocampal neurons. J Neurosci. 31:2721–2733

DiGiovanni J, Sun T, Sheng ZH, 2012. Characterizing synaptic vesicle proteins using synaptosomal fractions and cultured hippocampal neurons.Curr Protoc Neurosci. Chapter 2:Unit 2.7.1-22.

Fiala JC, Feinberg M, Popov V, Harris KM., 1998. Synaptogenesis via dendritic filopodia in developing hippocampal area CA1.J Neurosci. 18:8900-8911.

Galeano P, Blanco Calvo E, Madureira de Oliveira D, Cuenya L, Kamenetzky GV, Mustaca AE, Barreto GE, Giraldez-Alvarez LD, Milei J, Capani F, 2011. Long-lasting effects of perinatal asphyxia on exploration, memory and incentive downshift. International journal of developmental neuroscience Int J Dev Neurosci. 29:609-619.

Griffin RJ, Moloney A, Kelliher M, Johnston JA, Ravid R, Dockery P, O'Connor R, O'Neill C., 2005. Activation of Akt/PKB, increased phosphorylation of Akt substrates and loss and altered distribution of Akt and PTEN are features of Alzheimer's disease pathology. Journal Neurochem. 93:105-117.

Harrison PJ., 2004. The hippocampus in schizophrenia: a review of the neuropathological evidence and its pathophysiological implications. Psychopharmacology. 174:151-162.

Hoffman GE., Moore N, Fiskum G, Murphy AZ., 2003. Ovarian steroid modulation of seizure severity and hippocampal cell death after kainic acid treatment. Exp. Neurol. 124–134.

Huang BY, Castillo M. Hypoxic-ischemic brain injury: imaging findings from birth to adulthood. Radiographics : a review publication of the Radiological Society of North America, Inc 2008;28:417-439; quiz 617.

Johnston MV., 2004. Clinical disorders of brain plasticity.Brain & development. 26:73-80.

Johnston MV, 2011. Education of a child neurologist: developmental neuroscience relevant to child neurology. SeminPediatr Neurol. 133-138.

Kaech S, Fischer M, Doll T, Matus A., 1997. Isoform specificity in the relationship of actin to dendritic spines.J Neurosci. 17:9565-9572.

Kwon CH, Luikart BW, Powell CM, Zhou J, Matheny SA, Zhang W, Li Y, Baker SJ, Parada LF., 2006. Pten regulates neuronal arborization and social interaction in mice. Neuron. 50:377-388.

Lorenzini, C. A., Baldi, E., Bucherelli, C., Sacchetti, B., &Tassoni, G., 1996. Role of dorsal hippocampus in acquisition, consolidation and retrieval of rat's passive avoidance response: A tetrodotoxin functional inactivation study. Brain Research, 730, 32–39.

Martinez-Tellez RI, Hernandez-Torres E, Gamboa C, Flores G., 2009. Prenatal stress alters spine density and dendritic length of nucleus accumbens and hippocampus neurons in rat offspring. Synapse. 63:794-804.

Matus A., 2000. Actin-based plasticity in dendritic spines. Science. 290:754-758.

McGann JC, Lioy DT, Mandel G. Astrocytes conspire with neurons during progression of neurological disease. Current opinion in neurobiology 2012;22:850-858.

Meredith RM, Dawitz J, Kramvis I., 2012. Sensitive time-windows for susceptibility in neurodevelopmental disorders.Trends Neurosci. 35:335-344.

Monteleone MC, Adrover E, Pallares ME, Antonelli MC, Frasch AC, Brocco MA., 2013. Prenatal stress changes the glycoprotein GPM6A gene expression and induces epigenetic changes in rat offspring brain. Epigenetics. 1:152-160.

Morales P, Fiedler JL, Andrés S, Berrios C, Huaiquín P, Bustamante D, Cardenas S, Parra E, Herrera-Marschitz M., 2008. Plasticity of hippocampus following perinatal asphyxia: effects on postnatal apoptosis and neurogenesis. J Neurosci Res. 86:2650-2662.

Muñiz J, Romero J, Holubiec M, Barreto G, González J, Saint-Martin M, Blanco E, Cavicchia CJ, Castilla R, Capani F.,2014. Neuroprotective effects of hypothermia on synaptic actin cytoskeletal changes induced by perinatal asphyxia. Brain Res. 1563:1581-90.

Mychasiuk R, Gibb R, Kolb B., 2012. Prenatal stress alters dendritic morphology and synaptic connectivity in the prefrontal cortex and hippocampus of developing offspring. Synapse. 66:308-314.

Newey SE, Velamoor V, Govek EE, Van Aelst L., 2005. Rho GTPases, dendritic structure, and mental retardation.J Neurobiol. 64:58-74.

Ordy JM, Wengenack TM, Bialobok P, et al. Selective vulnerability and early progression of hippocampal CA1 pyramidal cell degeneration and GFAP-positive astrocyte reactivity in the rat four-vessel occlusion model of transient global ischemia. Experimental neurology 1993;119:128-139.

Pokorny J, Yamamoto T., 1981. Postnatal ontogenesis of hippocampal CA1 area in rats. I. Development of dendritic arborisation in pyramidal neurons. Brain research bulletin. 7:113-120.

Rami A, Jansen S, Giesser I, Winckler J., 2003. Post-ischemic activation of caspase-3 in the rat hippocampus: evidence of an axonal and dendritic localisation. Neurochem Int. 43:211-223.

Robertson CL, Puskar A, Hoffman GE, Murphy AZ, Saraswati M, Fiskum G., 2006. Physiologic progesterone reduces mitochondrial dysfunction and hippocampal cell loss after traumatic brain injury in female rats. Exp Neurol. 197:235-243.

Rojas DC, Smith JA, Benkers TL, Camou SL, Reite ML, Rogers SJ., 2004. Hippocampus and amygdala volumes in parents of children with autistic disorder.Am J Psychiatry. 161:2038-2044.

Roozendaal, B., Brunson, K.L., Holloway, B.L., McGaugh, J.L., Baram, T.Z., 2002. Involvement of stress-released corticotropin-releasing hormone in the basolateral amygdale in regulating memory consolidation. Proc. Natl. Acad. Sci. U. S. A. 99 (21), 13908–13913.

Saraceno GE, Bertolino ML, Galeano P, Romero JI, Garcia-Segura LM, Capani F., 2010. Estradiol therapy in adulthood reverses glial and neuronal alterations caused by perinatal asphyxia. Exp Neurol. 223:615-622.

Saraceno GE, Castilla R, Barreto GE, Gonzalez J, Kolliker-Frers RA, Capani F., 2012. Hippocampal dendritic spines modifications induced by perinatal asphyxia.Neural plasticity.2012:873532.

van Handel M, Swaab H, de Vries LS, Jongmans MJ.,2007. Long-term cognitive and behavioral consequences of neonatal encephalopathy following perinatal asphyxia: a review. Eur J Pediatr. 166:645-654.

Vereczki V, Martin E, Rosenthal RE, Hof PR, Hoffman GE, Fiskum G., 2006.Normoxic resuscitation after cardiac arrest protects against hippocampal oxidative stress, metabolic dysfunction, and neuronal death. J Cereb Blood Flow Metab. 6:821-835.

Weibel, E. R., 1979. Stereological Methods.Practical Methods for Biological Morphometry, Vol. I. Academic Press, New York.

Yoshihara Y, De Roo M, Muller D., 2009. Dendritic spine formation and stabilization. Curr Opin Neurobiol. 19:146-153.

Ziv NE, Smith SJ, 1996. Evidence for a role of dendritic filopodia in synaptogenesis and spine formation. Neuron. 17:91-102.

FIGURE LEGENDS

Figure 1.Neuronal alterations induced by PA. a) Micrographs of *Stratum radiatum* of CA1 hippocampal area from one-month-old control rats and rats subjected to 19min of PA.

Sections of 50 μm were analyzed by NeuN immunostaining (left) and electron microscopy (EM) (right). Abnormal NeuN+ nuclei (arrow) were increased in asphyctic group respect to control one (inset). Electron micrograph showed that most of the condensed cells correspond to neurons in degeneration (arrows). Confocal microscope images of GFAP immunostaining showed no morphological alterations between groups (inset). Scale bars: 30 μm and 0.5 μm for EM. Nu: nucleus. **b)** Statistical assessment of different parameters analyzed. At least three independent experiments were analyzed. Significant differences were determined by Student *t*-test. *p<0.05.

Figure 2. β-actin expression and dendritic spine density were affected by PA. a) *β-actin* mRNA levels were determined by real time RT-PCR and normalized to the reference gene *cyclophilin*. *p<0.05. Bars and error bars represent mean ± SEM. Statistical analyses were determined by Student *t*-test. **b)** Immunoblots of hippocampal synaptosomal fraction of one-month-old control and asphyctic rats. Glyceraldehyde-3-phosphate dehydrogenase (GAPDH) content was used as loading control. *p<0.05. **c)** Confocal microscopy images of Phalloidin-Alexa^{568} staining from *Stratum radiatum* of CA1 hippocampal tissue from control and PA groups. An increase in the punctate staining was observed after 19 minutes of PA (arrows) (**p<0.01). Scale bar: 10 μm. Electron micrographs of photooxidated *Stratum radiatum* from CA1 hippocampal area of 30-day-old rats. Arrows point out the dendritic spines stained. (**p<0.01). Scale bar: 1 μm.

Figure 3. Filopodium and M6a expression enhancement induced by PA. a) Electron micrograph of filopodia. The magnification of a filopodium allows us to observe its long structure and the parenteral dendrites (arrows). Scale bar: 1 μm. **b)** *Gpm6a* mRNA level in the hippocampus determined by real time RT-qPCR. *Gpm6a* values were normalized with the reference gene *cyclophilin*. *p<0.05.**c)** Fluorescence microscope images of M6a immunostaining from *Stratum radiatum* of CA1 hippocampal tissue from one-month-old control and PA rats (arrows). An increase in the punctate staining was observed in asphyctic animals (inset). **p<0.01. Bars and error bars represent mean ±SEM. Statistical analyses were determined by Student *t*-test. Scale bar: 10 μm.

Figure 4. Up-regulation of PI3K/Akt/GSK3 activity induced by PA. Representative Western blot showing p-Akt, Akt, GSK3-p-Ser9 and GSK3 expression. *p<0.05. Inset: Cellular localization of pAkt in both groups. We could observe that the expression is mainly located in CA1 pyramidal neurons. Scale bars: 30 μm. Bars and error bars represent mean ± SEM. Statistical analyses were determined by Student t-test.

Figure 5.Locomotor activity and exploratory behavior in the open field test. Experimental groups: Control rats (CTL, n = 8) and rats subjected to perinatal asphyxia (PA, n = 8). The first and second bar of each group corresponds to the first and second exposure to the OF, respectively. Statistical analyses were carried out by one-way analysis of variance (ANOVA) followed by post-hoc multiple comparisons (Fisher´s test). Data are expressed as mean+ SEM. **a)** Both groups showed a significantly reduced total number of lines crossed when they were re-exposed to the OF. Note that asphyctic animals showed a more pronounced decrement compared with CTL animals. **p<0.01, ***p<0.001.**b)** Asphyctic animals showed a significant increase in the grooming time parameter during the

second exposure to the OF. **p<0.01.**c)** Regarding the duration of grooming episodes, there was a significant increase during the second exposure to the OF in the PA group, and between the second exposure of PA group respect to the second exposure from CTL group. *p< 0.05; **p<0.01.**d)** Taking into account the percentage of time parameter, PA group presented a significant decrease in phase I and a significant increase in the second one compared to the CTL group. *p<0.05.**e)** Statistically significant correlation between number of lines crossed and total grooming time in asphyctic animals.R^2=0.6863. **p<0.01.**f)** Statistically significant correlation between number of lines crossed and total grooming time during the second exposure to the OF in asphyctic animals. R^2=0.4728. *p< 0.05.

SUPPLEMENTAL MATERIAL

Legends

Figure 1. Perinatal asphyxia does not alter process morphology. Optical microscopy images of MAP-2 and pH/M NF immunostaining from *Stratum radiatum* of CA1 hippocampal area. No obvious differences in MAP-2 (arrows) immunostaining (a)neitherin the phosphorylation status of medium and heavy neurofilaments (pH/M NF) (arrows) immunostaining (b) were observed between PA and CTL groups. Bars and error bars represent mean ± SEM. Statistical analyses were determined by Student *t*-test. Scale bar: 50 μm.

Figure 2.a). Time in the center in the OF test. No significant differences were observed between groups (p = 0 .7957, n.s.). **b).** Latency in the center in the OF test. No significant differences were observed between groups in the first exposure to the OF. Statistical analyses were determined by Student t-test. Data are expressed as mean ± SEM.

Figure3. Associated memory in the inhibitory avoidance test. No differences were observed between groups in the ratio T1/T2 (T2/T1) (p = 0.240, n.s.). Statistical analyses were determined by Student t-test. Data are expressed as mean ± SEM.

a)

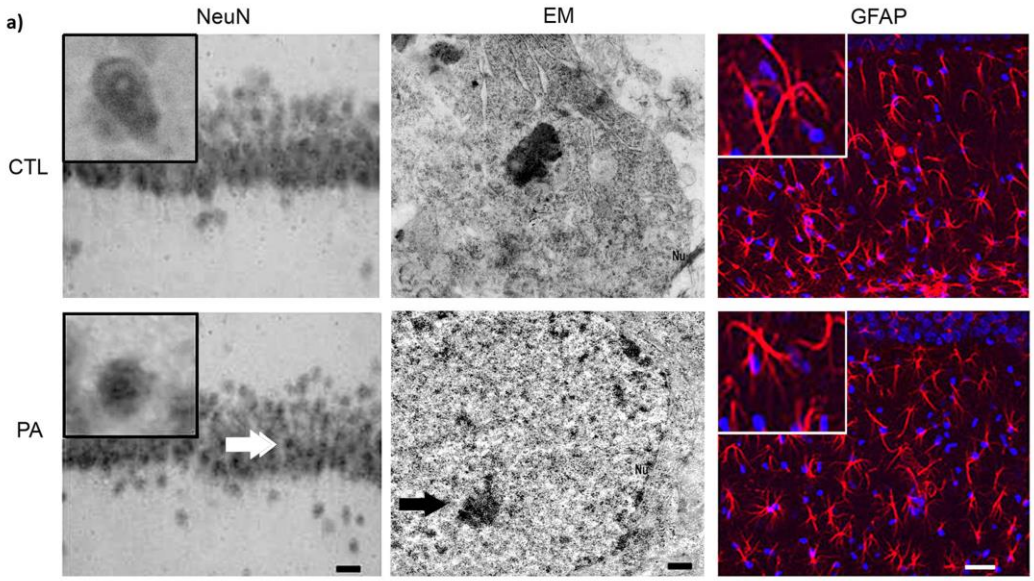

b)

Groups	Pyknotic nuclei	Neurons NeuN+	Normal Neurons	Abnormal neurons	Number of astrocytes GFAP+/mm^3
CTL	14.62 ± 1.2	75.34 ± 2.4	72.20 ± 0.5	3.04 ± 0.5	8300 ± 303
PA	20.96 ± 0.3 *	61.32 ± 5.5	50.44 ± 0.9	10.88 ± 0.6 *	10037 ± 154

Data are expressed as means ± SD. Significative differences were obtain using Student t-test. *P < 0.05.

Fig. 1

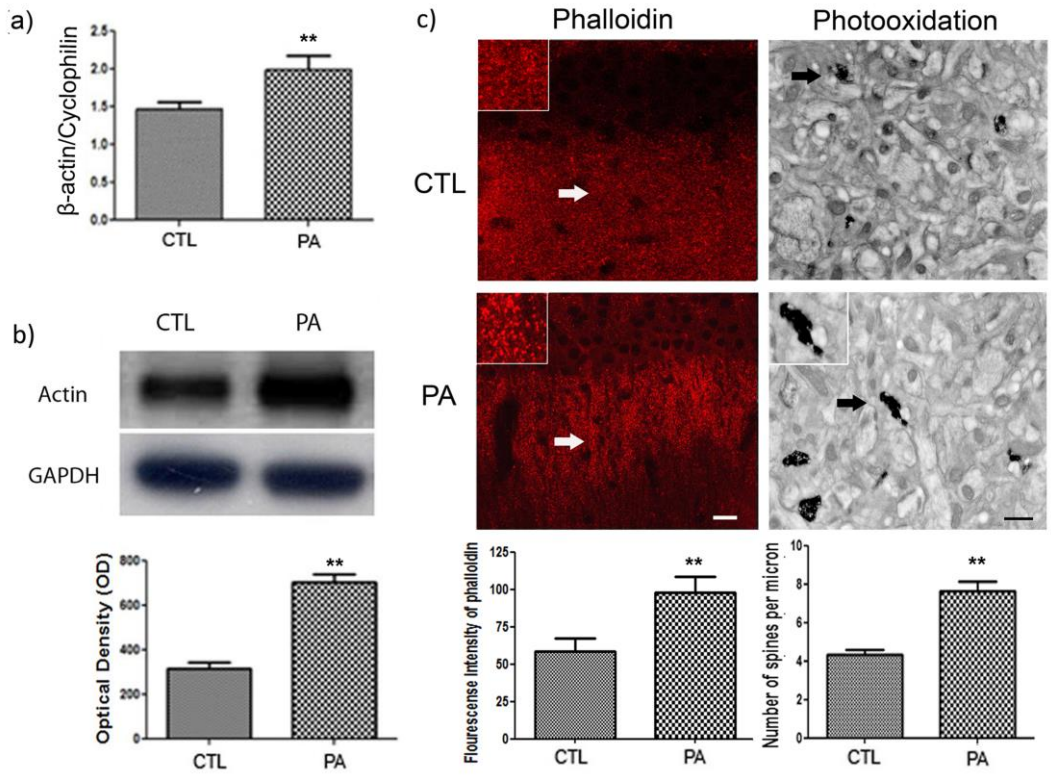

Fig. 2

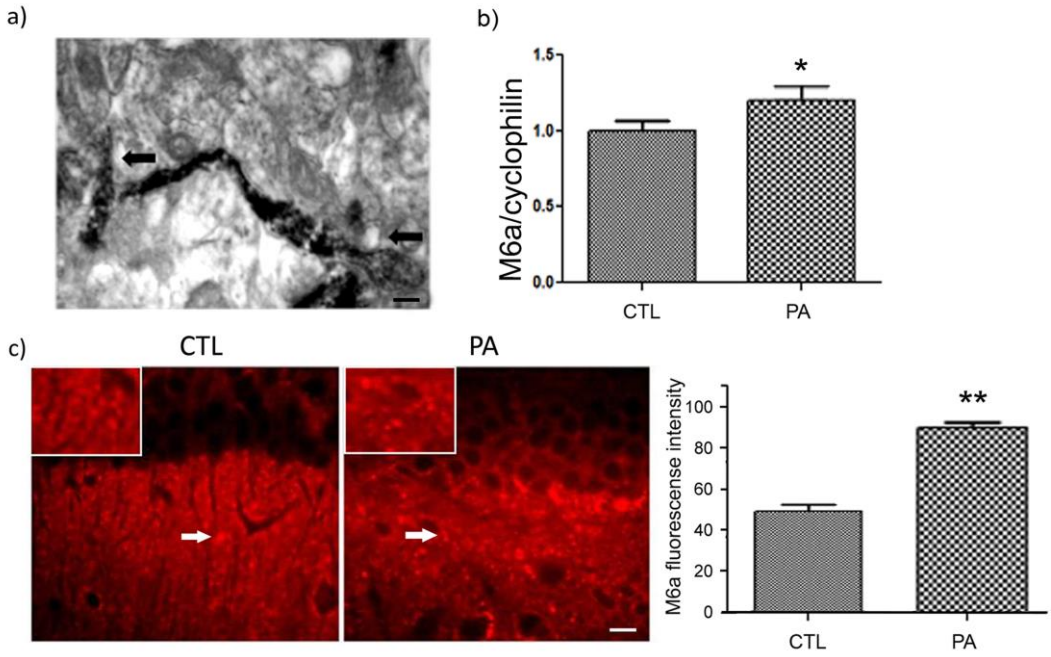

Fig. 3

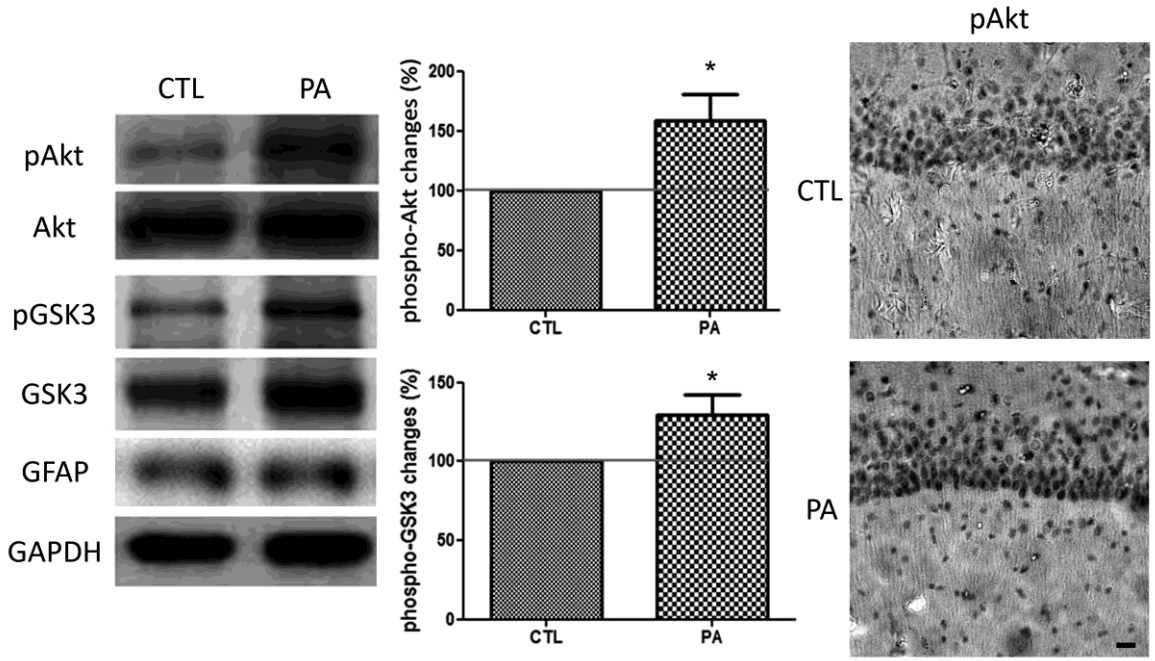

Fig. 4

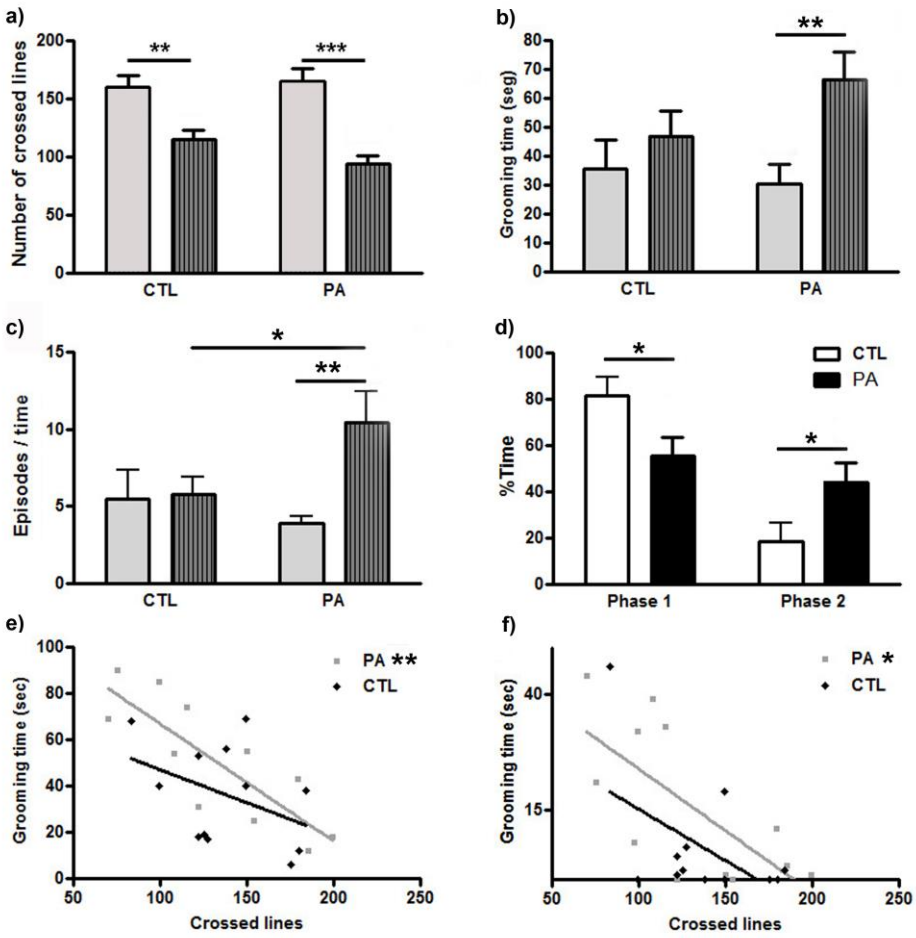

Fig. 5